Supplementary Information for

Multi-isotopic study of the earliest medieval inhabitants of Santiago de Compostela (Galicia, Spain)

Patxi Pérez-Ramallo[1,2,3*], Aurora Grandal-d´Anglade[4], Elia Organista[5,6], Elena Santos[7], David Chivall[8], Ricardo Rodríguez-Varela[9,10], Anders Götherström[9,10], Francisco Etxeberria[3], Jana Ilgner[1,2], Ricardo Fernandes[1,11,12], Juan Luis Arsuaga[13], Petrus Le Roux[14], Tom Higham[15], Julia Beaumont[16], Hannah Koon[16], Patrick Roberts[1,2,17*]

[1]isoTROPIC Research Group, Max Planck Institute for Geoanthropology. Kahlaische Str. 10, 07745, Jena, Germany.

[2]Department of Archaeology, Max Planck Institute for Geoanthropology. Kahlaische Str. 10, 07745, Jena, Germany.

[3]Departamento de Especialidades Médico-Quirúrgicas, Facultad de Medicina y Enfermería, University of the Basque Country (EHU), Donostia-San Sebastián, Spain.

[4]Instituto Universitario de Xeoloxía, Universidade da Coruña (UDC). ESCI. 15071, A Coruña, Spain.

[5]Osteoarcheological Research Laboratory. Department of Archaeology and Classical Studies, Stockholm University, 106 91, Stockholm, Sweden.

[6]Institute of Evolution in Africa (IDEA), University of Alcalá de Henares, 28010, Madrid, Spain.

[7]University of Burgos (UBu), Burgos, Spain.

[8]Oxford Radiocarbon Accelerator Unit, Research Laboratory for Archaeology and the History of Art, University of Oxford, Oxford, OX13QY, United Kingdom.

[9]Centre for Palaeogenetics, 106 91, Stockholm, Sweden

[10]Department of Archaeology and Classical Studies, Stockholm University, 10691, Stockholm, Sweden.

[11] Climate Change and History Research Initiative, Princeton University, Princeton, USA.

[12]Faculty of Arts, Masaryk University, Brno, Czech Republic.

[13]Universidad Complutense de Madrid. Centro Mixto UCM-ISCIII, Madrid, Spain.

[14]Dept of Geological Sciences, University of Cape Town, Cape Town, Sourth Africa

[15]Research Network Human Evolution and Archaeological Sciences (HEAS), Department of Evolutionary Anthropology, University of Vienna, Vienna, Austria.

[16]School of Archaeological and Forensic Sciences, Faculty of Life Sciences, University of Bradford, Bradford, United Kingdom.

[17]School of Social Sciences, University of Queensland, St Lucia QLD 4072, Brisbane, Australia.

*correspondence to: Patxi Pérez-Ramallo (ramallo@shh.mpg.de) and Patrick Roberts (roberts@shh.mpg.de)

This PDF file includes:

Supplementary Text S1. Radiocarbon dating method:

S1.1 Oxford Radiocarbon Accelerator Unit (ORAU): human and animal bone from the fauna found in tomb NCS146, individuals bone or teeth NCS154, NCS258b, NCS030, and NCS023; were radiocarbon dated at the Oxford Radiocarbon Accelerator Unit (ORAU). Prior to extensive sampling of human skeletal remains we screened small (3–5 mg) sub-samples of drilled bone powder by measuring the elemental nitrogen concentration. This is a useful proxy for protein, and therefore presence of collagen in the bone (Brock et al. 2010; Jacob et al. 2018). Samples with >~0.5%N were passed for full collagen extraction treatment for AMS dating. The methods used are outlined in Brock et al. 2010. Briefly, collagen was extracted using an acid-base-acid procedure followed by gelatinization and lyophilization (Brock et al. 2010). The extracted gelatin was filtered using pre-cleaned Vivaspi 30kD MWCO ultra-filters (Brown et al. 1988; Higham et al. 2006). Ultrafiltration removes low molecular weight contaminants and produces a better purified collagen fraction as indicated by improved C:N atomic ratios and carbon mass on combustion. The filtered collagen was freeze-dried and combusted in a CHN analyser linked in continuous flow mode to a Europa isotope ratio mass spectrometer (EA-CF-IRMS) using a He carrier gas. $\delta^{13}C$ and $\delta^{15}N$ values, nitrogen and carbon content, and bone C:N atomic ratios were determined. The purified CO_2 was then reduced to graphite using H_2 in a reaction catalysed by 2 mg of a Fe powder at 560°C for 6 hr. The graphite was pressed into an Al target holder prior to radiocarbon measurement using AMS (Bronk Ramsey et al. 2004). We tested the reliability of dating bone with collagen yields of this size and the models showed that none were outliers. All other analytical parameters measured, including the carbon to nitrogen atomic ratio, were acceptable. We therefore consider the results to be robust. The calibration and the calibration curve were performed by OxCal V4.4 Bronk Ramsey (2017): r.5: IntCarl20 atmospheric curve (Reimer et al. 2020).

S1.2 Beta Analytic: We sent to radiocarbon dated human bone from individuals NCS005 and NCS007. Before radiocarbon dating, the samples were first gently crushed then dispersed in deionized water. They were then washed with hot HCl acid to eliminate carbonates followed by an alkali wash (NaOH) to remove secondary organic acids. The alkali wash is followed by a final acid rinse to neutralize the solution before drying. After this, the samples for radiocarbon dating were bathed in sodium chlorite (NaClO2) under controlled conditions (pH 3 and temperature at 70°C). The AMS measurement was done on graphite produced by hydrogen reduction of the CO_2 sample over a cobalt catalyst. The CO_2 was obtained from the combustion of the sample at 800°C+ under a 100% oxygen atmosphere. The CO_2 is first dried with methanol/dry ice then collected in liquid nitrogen for the subsequent graphitization reaction. The identical reaction is performed on reference standards, internal QA samples, and backgrounds to ensure systematic chemistry. The analytical results ("BP" or "pMC") were obtained by measuring sample C^{14}/C^{13} relative to the C^{14}/C^{13} in Oxalic Acid II (NIST-4990C) in one of Beta Analytic's multiple in-house particle accelerators using SNICS ion source. Quality assurance samples were measured along with the unknowns and reported separately. The AMS results have been corrected for total fractionation using machine graphite $\delta^{13}C$. The IRMS performs the separation and measurement of the CO_2 masses (44, 45, and 46) and calculation of the sample $\delta^{13}C$.

Figure S2. δ^{13}C and δ^{15}N of teeth (Incremental Dentine Technique) and ribs from the same individuals at the Medieval Necropolis of the Cathedral of Santiago analysed at the University of Bradford in 2015 following Beaumont et al. (2013)

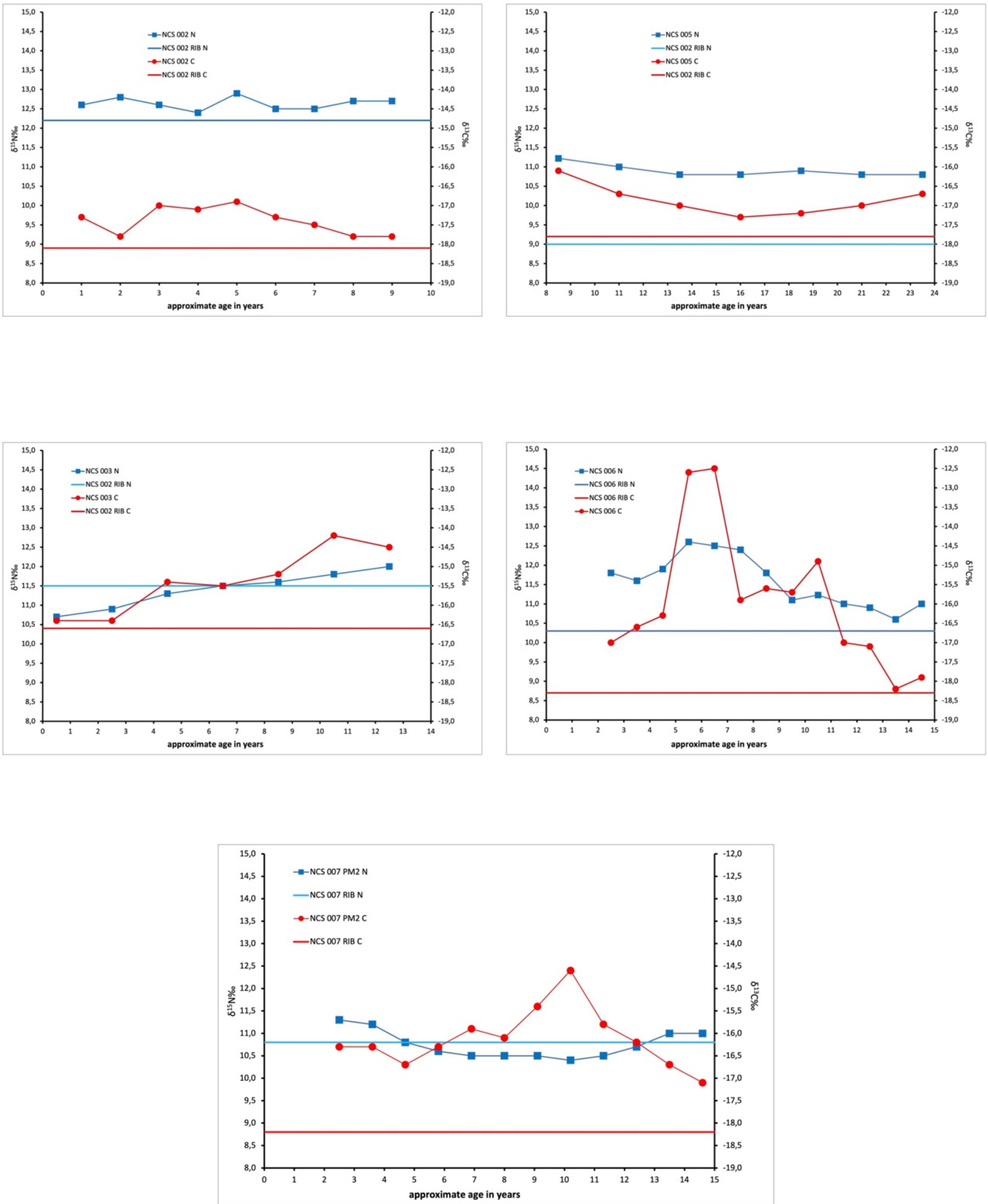

Figure S3. Map of $\delta^{18}O_{dw}$ modern local meteoric water made following data from Araguas-Araguasa and Diaz Teijeiro (2005). The map was created using the sowtware Adobe Illustrator 24.3 from ArcGis server for MAGNA (https://www.adobe.com/products/illustrator.html)

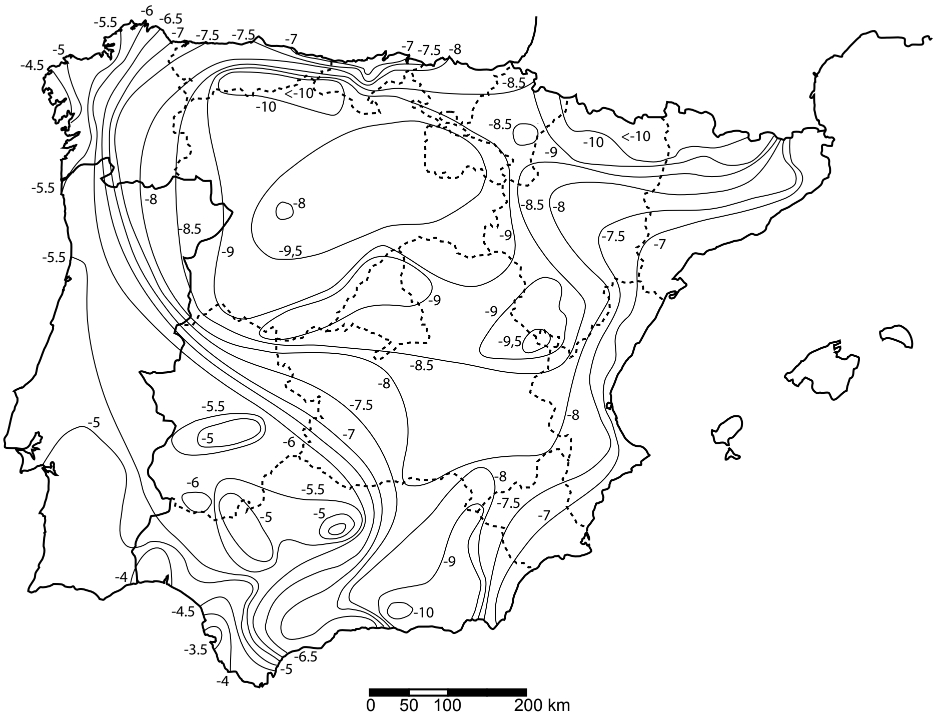

Figure S4. δ^{13}C and δ^{15}N of teeth (second molars, except for individual NCS032) and ribs from the same individuals at the Medieval Necropolis of the Cathedral of Santiago. T= tooth (triangles); R= Rib (circles); P-II= Phase II (10th-11th centuries AD); P-III= Phase III (11th-12th centuries AD)

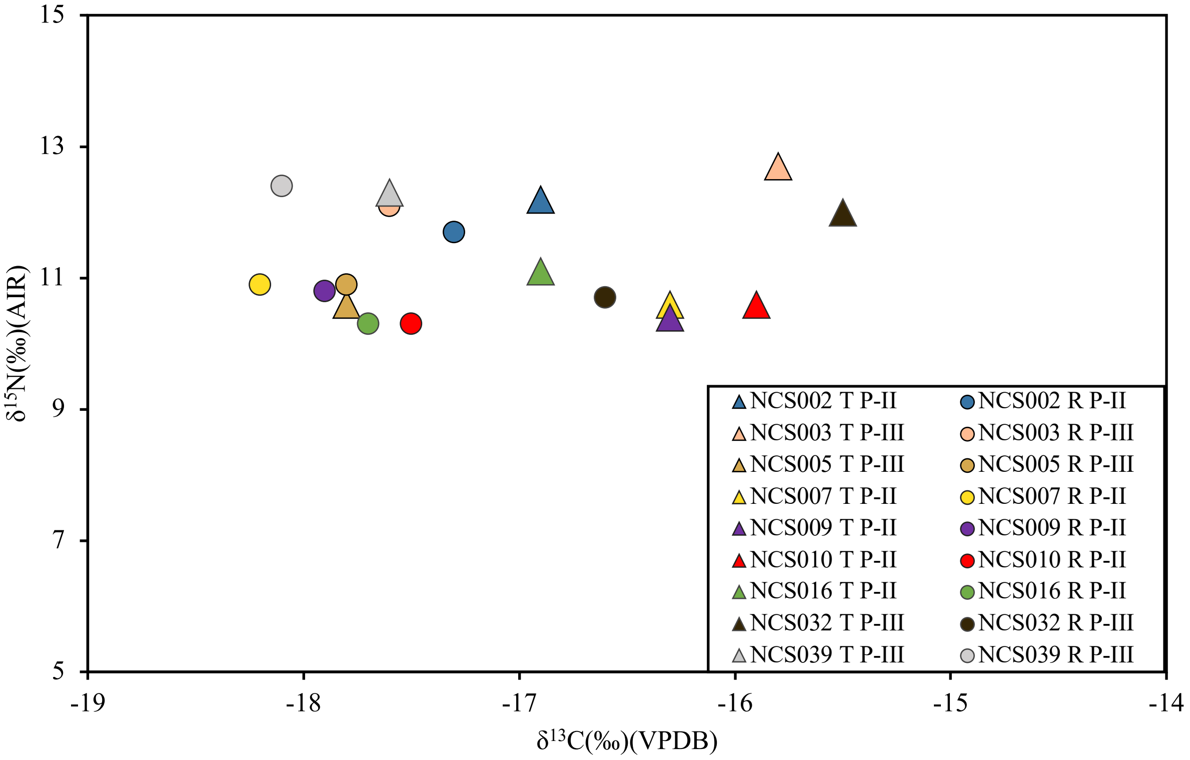

114 **Figure S5. $\delta^{13}C_{ap}$, $\delta^{15}N_{coll}$, $\delta^{13}C_{coll}$, and $\delta^{18}O_{ap}$ of tooth enamel and dentine of humans of**
115 **the present study**

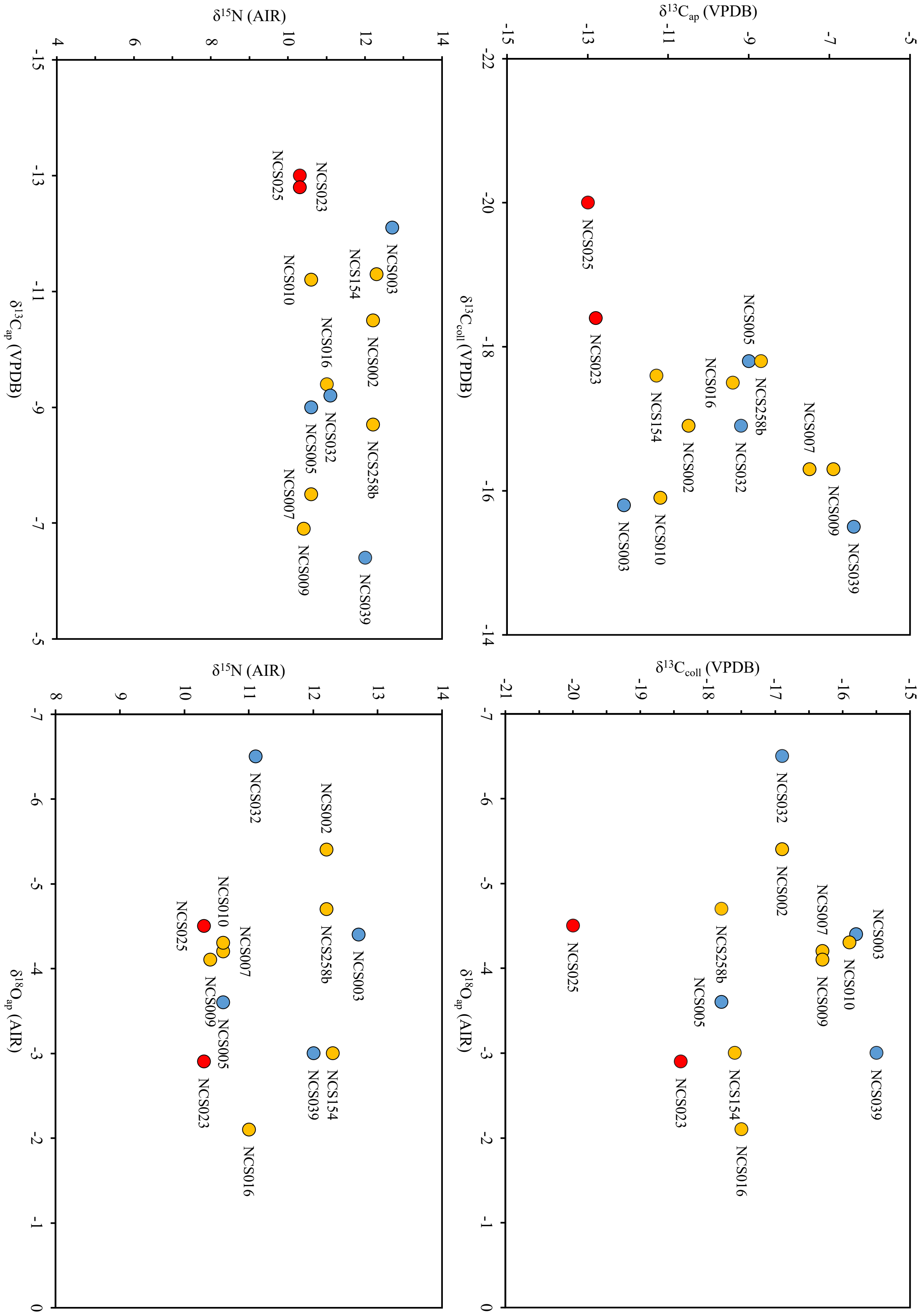

116

Table S1. Human incremental dentine $\delta^{13}C$ and $\delta^{15}N$ stable isotope data, and enamel carbonate $\delta^{18}O_{ap}$ and $\delta^{13}C_{ap}$ analysed at the University of Bradford (Bradford, the UK) (Pérez Ramallo 2015)

Reference	$\delta^{15}N$ (‰)	$\delta^{13}C$ (‰)	Age	Crown Mean	Enamel $\delta^{18}O_{ap}$ Carbonate	Enamel $\delta^{13}C_{ap}$ Carbonate
NCS001	NCS001	NCS001	NCS001	NCS001	NCS001	NCS001
-	-	-	-	-	25.6 (Incisor)	-14.4 (Incisor)
NCS002	NCS002	NCS002	NCS002	NCS002	NCS002	NCS002
NCS002 1	-17.3	12.6	2.5	-17.4	25.2 (Second Molar)	-12.7 (Second Molar)
NCS002 2	-17.8	12.8	4.0	-	-	-
NCS002 3	-17.0	12.6	5.5	-	-	-
NCS002 4	-17.1	12.4	7.0	-	-	-
NCS002 5	-16.9	12.9	8.5	-	-	-
NCS002 6	-17.3	12.5	10.0	-	-	-
NCS002 7	-17.5	12.5	11.5	-	-	-
NCS002 8	-17.8	12.7	13.0	-	-	-
NCS002 9	-17.8	12.7	14.5	-	-	-
NCS003	NCS003	NCS003	NCS003	NCS003	NCS003	NCS003
NCS003 1	-16.4	10.7	0.5	-16.1	25.8 (Second Molar)	-8.7 (Second Molar)
NCS003 2	-16.4	10.9	2.5	-	-	-
NCS003 3	-15.4	11.3	4.5	-	-	-
NCS003 4	-15.5	11.5	6.5	-	-	-
NCS003 5	-15.2	11.6	8.5	-	-	-
NCS003 6	-14.2	11.8	10.5	-	-	-
NCS003 7	-14.5	12.0	12.5	-	-	-
NCS004	NCS004	NCS004	NCS004	NCS004	NCS004	NCS004
-	-	-	-	-	28.1 (Second Molar)	-8.7 (Second Molar)
NCS005	NCS005	NCS005	NCS005	NCS005	NCS005	NCS005
NCS005 1	-16.1	11.2	8.5	-16.6	25.6 (Third Molar)	-10.2 (Third Molar)
NCS005 2	-16.7	11.0	11.0	-	-	-
NCS005 3	-17.0	10.8	13.5	-	-	-
NCS005 4	-17.3	10.8	16.0	-	-	-
NCS005 5	-17.2	10.9	18.5	-	-	-
NCS005 6	-17.0	10.8	21.0	-	-	-
NCS005 7	-16.7	10.8	23.5	-	-	-
NCS006	NCS006	NCS006	NCS006	NCS006	NCS006	NCS006
NCS006 1	-17.0	11.8	2.5	-16.6	25.3 (Second Molar)	-9.0 (Second Molar)
NCS006 2	-16.6	11.6	3.5	-	-	-
NCS006 3	-16.3	11.9	4.5	-	-	-
NCS006 4	-12.6	12.6	5.5	-	-	-
NCS006 5	-12.5	12.5	6.5	-	-	-
NCS006 6	-15.9	12.4	7.5	-	-	-
NCS006 7	-15.6	11.8	8.5	-	-	-
NCS006 8	-15.7	11.1	9.5	-	-	-
NCS006 9	-14.9	11.2	10.5	-	-	-
NCS006 10	-17.0	11.0	11.5	-	-	-
NCS006 11	-17.1	10.9	12.5	-	-	-
NCS006 12	-18.2	10.6	13.5	-	-	-
NCS006 13	-17.9	11.0	14.5	-	-	-
NCS007	NCS007	NCS007	NCS007	NCS007	NCS007	NCS007
NCS007 Mo 1	-16.3	10.9	2.5	-16.1	26.8	-8.4

					(Second Molar)	(Second Molar)
NCS007 Mo 2	-15.6	10.9	3.7			
NCS007 Mo 3	-16.4	10.6	4.9			
NCS007 Mo 4	-16.0	10.3	6.1			
NCS007 Mo 5	-15.4	10.4	7.3			
NCS007 Mo 6	-14.8	10.3	8.5			
NCS007 Mo 7	-15.8	10.2	9.7			
NCS007 Mo 8	-16.0	10.3	10.9			
NCS007 Mo 9	-15.9	10.7	12.1			
NCS007 Mo 10	-15.8	10.9	13.3			
NCS007 Mo 11	-15.7	11.0	14.5			
NCS009	NCS009	NCS009	NCS009	NCS009	NCS009	NCS009
NCS009	-	-	-	-	27.6 (Molar)	-9.3 (Molar)

Table S2. Radiocarbon determinations, $\delta^{13}C$ measured at time of collection for radiocarbon determination, and calibrated ages. Calibrated using OxCal. v4.4 Bronk Ramsey (2021) and the IntCal20 atmospheric curve (Reimer et al. 2020)

Lab code	Sample Reference	Location	Material	Radiocarbon years before present (BP)	$\delta^{13}C$ (‰)	Calibrated calendar date (95.4%)
OxA-38165	NCS146	Zone 1 necropolis Cathedral of Santiago. Tomb type “Sarcophagus”.	Bone *Bos taurus*	1167±26	-21.7	772-974 cal AD
OxA-38017	NCS154	Zone 1 Necropolis Cathedral of Santiago. Tomb type “Cists”	Tooth *Homo sapiens*	1119±24	-17.3	886-992 cal AD
OxA-37968	NCS258b	Zone 2 Necropolis Cathedral of Santiago. Tomb type “Anthropomorphic”	Tooth *Homo sapiens*	1008±25	-17.9	991-1150 cal AD
Beta-477850	NCS007	Zone 0 Necropolis Cathedral of Santiago. Tomb type “Anthropomorphic”	Tooth *Homo sapiens*	980±30	-18.4	995-1158 cal AD
OxA-38173	NCS009	Zone 0 Neropolis Cathedral of Santiago. Tomb type “Anthropomorphic”	Tooth *Homo sapiens*	1014±26	-16.9	990-1150 cal AD
OxA- 38175	NCS030	Zone 0 Necropolis Cathedral of Santiago. Tomb type “Cists”	Bone *Homo sapiens*	1036±27	-18.3	899-1040 cal AD
OxA-38174	NCS030	Zone 0 Necropolis Cathedral of Santiago. Tomb type “Cits”	Bone *Homo sapiens*	999±28	-18.2	992-1153 cal AD
OxA-38164	NCS023	Zone 0 Necropolis Cathedral of Santiago. Tomb type “Sarcophagus”	Tooth *Homo sapiens*	1195±26	-18.3	710-943 cal AD
Beta-477849	NCS005	Zone 0 Necropolis Cathedral of Santiago. Tomb type “Rectangular”	Bone *Homo sapiens*	940±30	-17.8	1028-1172 cal AD

Table S3. Human δ^{13}C and δ^{15}N stable isotope ratios, collagen quality indicators, location, and chronology

Reference	Place	Chronology	Sample	δ^{15}N (‰)	δ^{13}C (‰)	%N	%C	C/N	Collagen Yield (%)
NCS001	Cathedral of Santiago de Compostela (Galicia)	9th-12th centuries AD	Rib	8.7	-19.8	14.7	40.0	3.2	3.5
NCS002	Cathedral of Santiago de Compostela (Galicia)	9th-12th centuries AD	LM$_2$	12.2	-16.9	15.6	43.6	3.2	18.3
NCS002	Cathedral of Santiago de Compostela (Galicia)	9th-12th centuries AD	Rib	11.7	-17.3	15.2	41.8	3.2	20.2
NCS003	Cathedral of Santiago de Compostela (Galicia)	9th-12th centuries AD	LM$_2$	12.7	-15.8	12.9	39.3	3.5	10.3
NCS003	Cathedral of Santiago de Compostela (Galicia)	9th-12th centuries AD	Rib	12.1	-17.6	2.5	7.6	3.5	5.8
NCS005	Cathedral of Santiago de Compostela (Galicia)	9th-12th centuries AD	LM$_2$	10.6	-17.8	15.8	43.5	3.2	8.2
NCS005 (Rejected)	Cathedral of Santiago de Compostela (Galicia)	9th-12th centuries AD	Canine	14.8	-17.4	7	33.5	5.6	0.7
NCS005	Cathedral of Santiago de Compostela (Galicia)	9th-12th centuries AD	Rib	10.9	-17.8	14.9	42.4	3.3	18.9
NCS006aB	Cathedral of Santiago de Compostela (Galicia)	9th-12th centuries AD	Rib	10.5	-17.8	12.9	35.2	3.2	12.3
NCS006b	Cathedral of Santiago de Compostela (Galicia)	9th-12th centuries AD	Femur	10.6	-17.4	12.9	35.2	3.2	2.3
NCS007	Cathedral of Santiago de Compostela (Galicia)	9th-12th centuries AD	LM^2	10.6	-16.3	15.3	41.2	3.1	5.8
NCS007	Cathedral of Santiago de Compostela (Galicia)	9th-12th centuries AD	Rib	10.9	-18.2	15.9	44.1	3.2	15.8
NCS008	Cathedral of Santiago de Compostela (Galicia)	9th-12th centuries AD	Skull, right parietal	11.5	-18.3	15.5	42.6	3.2	12.4
NCS008	Cathedral of Santiago de Compostela (Galicia)	9th-12th centuries AD	Rib	11.6	-18.2	8.3	22.4	3.2	7.5
NCS009	Cathedral of Santiago de Compostela (Galicia)	9th-12th centuries AD	LM^2	10.4	-16.3	16.5	43.6	3.1	15.7
NCS009	Cathedral of Santiago de Compostela (Galicia)	9th-12th centuries AD	Rib	10.8	-17.9	16.3	44.5	3.2	1.1
NCS010	Cathedral of Santiago de	9th-12th centuries AD	RM^2	10.6	-15.9	15.9	43.9	3.2	9.6

	Compostela (Galicia)								
NCS010	Cathedral of Santiago de Compostela (Galicia)	9th-12th centuries AD	Rib	10.3	-17.5	15.6	43.1	3.2	20.6
NCS011	Cathedral of Santiago de Compostela (Galicia)	9th-12th centuries AD	Rib	11.1	-18	15.8	43.3	3.2	13.7
NCS012	Cathedral of Santiago de Compostela (Galicia)	9th-12th centuries AD	Rib	10.3	-17	16	43.9	3.2	4.1
NCS014	Cathedral of Santiago de Compostela (Galicia)	9th-12th centuries AD	LM^2	-	-	-	-	-	-
NCS014	Cathedral of Santiago de Compostela (Galicia)	9th-12th centuries AD	Rib	11.5	-18.4	14.2	38.3	3.1	6.6
NCS016	Cathedral of Santiago de Compostela (Galicia)	9th-12th centuries AD	LM$_2$	11	-17.5	16.4	45.1	3.2	33.5
NCS016	Cathedral of Santiago de Compostela (Galicia)	9th-12th centuries AD	Rib	10.8	-17.8	13.1	36.2	3.2	18.7
NCS022 (No collagen)	Cathedral of Santiago de Compostela (Galicia)	9th-12th centuries AD	RM	-	-	-	-	-	-
NCS023	Cathedral of Santiago de Compostela (Galicia)	9th-12th centuries AD	RM$_2$	10.3	-18.4	16.7	45.9	3.2	15.1
NCS024a (Rejected)	Cathedral of Santiago de Compostela (Galicia)	9th-12th centuries AD	Rib	11.2	-20.5	1.8	8.7	5.6	7.2
NCS025	Cathedral of Santiago de Compostela (Galicia)	9th-12th centuries AD	LM$_2$	10.3	-20.0	15.3	45.7	3.5	11.6
NCS025 (No collagen)	Cathedral of Santiago de Compostela (Galicia)	9th-12th centuries AD	LM$_3$	-	-	-	-	-	-
NCS025 (Rejected)	Cathedral of Santiago de Compostela (Galicia)	9th-12th centuries AD	Rib	16.5	-20	2.5	14.2	6.5	2.6
NCS026 (No collagen)	Cathedral of Santiago de Compostela (Galicia)	9th-12th centuries AD	LM^3	-	-	-	-	-	-
NCS026 (Rejected)	Cathedral of Santiago de Compostela (Galicia)	9th-12th centuries AD	Rib	8.7	-18.2	0.9	3.3	4.1	0.8
NCS030	Cathedral of Santiago de Compostela (Galicia)	9th-12th centuries AD	Right 5th metatarsal	10	-17.8	14.5	39.7	3.2	13.5
NCS032	Cathedral of Santiago de Compostela (Galicia)	9th-12th centuries AD	LP^2	11.1	-16.9	16.5	45.8	3.2	29.7
NCS032	Cathedral of Santiago de Compostela (Galicia)	9th-12th centuries AD	Rib	10.3	-17.7	15.8	43.6	3.2	24.7

NCS033	Cathedral of Santiago de Compostela (Galicia)	9th-12th centuries AD	Rib	10.9	-16	16.5	45.7	3.2	3.5
NCS034	Cathedral of Santiago de Compostela (Galicia)	9th-12th centuries AD	Rib	-	-	-	-	-	-
NCS039	Cathedral of Santiago de Compostela (Galicia)	9th-12th centuries AD	RM^2	12	-15.5	8.4	23.5	3.3	19
NCS039	Cathedral of Santiago de Compostela (Galicia)	9th-12th centuries AD	Rib	10.7	-16.6	16.3	45.3	3.2	11.4
NCS145a (Rejected)	Cathedral of Santiago de Compostela (Galicia)	9th-12th centuries AD	LM_2	7.9	-24.2	0.2	1.2	6.2	5.1
NCS145b (Rejected)	Cathedral of Santiago de Compostela (Galicia)	9th-12th centuries AD	LM_3	14	-19.7	1.1	5.8	5.9	3.9
NCS153	Cathedral of Santiago de Compostela (Galicia)	9th-12th centuries AD	drm_2	14.1	-18.2	13.7	40.5	3.5	11.7
NCS154	Cathedral of Santiago de Compostela (Galicia)	9th-12th centuries AD	RP^2	12.3	-17.6	15.8	43.9	3.2	1.9
NCS154	Cathedral of Santiago de Compostela (Galicia)	9th-12th centuries AD	Rib	12.4	-18.1	15.4	42.5	3.2	5.3
NCS256	Cathedral of Santiago de Compostela (Galicia)	9th-12th centuries AD	Skull fragment	11.6	-17.2	9	26.2	3.4	14.4
NCS258a	Cathedral of Santiago de Compostela (Galicia)	9th-12th centuries AD	Skull fragment	11.9	-18.4	15.8	43.6	3.2	17.0
NCS258b	Cathedral of Santiago de Compostela (Galicia)	9th-12th centuries AD	RM_2	12.2	-17.8	16.4	44.5	3.2	5.8
NCS258b	Cathedral of Santiago de Compostela (Galicia)	9th-12th centuries AD	RM_3	12.1	-18.2	13.4	37.4	3.3	24
NCS259	Cathedral of Santiago de Compostela (Galicia)	9th-12th centuries AD	Skull fragment	11.4	-17.2	13.7	40.0	3.4	8.1

Table S4. $\delta^{13}C$, $\delta^{15}N$, $\delta^{18}O_{ap}$, $\delta^{13}C_{ap}$, $\delta^{18}O_{dw}$, $\delta^{13}C_{ap-coll}$, and $^{87}Sr/^{86}Sr$ human data mean ± SD and range (minimum to maximum), and statistical comparison (Mann-Whitney with Monte-Carlo Permutation) between zones, biological sexes, and teeth and ribs from the same individuals

	$\delta^{15}N$ and $\delta^{13}C$	$^{87}Sr/^{86}Sr$	$\delta^{18}O_{ap}$ and $\delta^{13}C_{ap}$
Zone 0	10.7±0.7 (8.7 to 12.1) -17.8±0.9 (-20 to -16) n=20	0.713132 (0.709236-0.716632) n=21	-4.0±1.1 (-6.5 to -2.1) -9.8±2.2 (-13 to -6.4) n=13
Zone 1-2	11.9±0.4 (11.4 to 12.3) -17.6±0.5 (-18.4 to -17.2) n=5	0.713211 (0.711426-0.71581) n=5	-3.8±0.8 (-4.7 to -3) -11.3±2.3 (-14.2 to -8.7) n=4
Statistical Comparison Zone 0 vs Zones 1-2 (p-value)	$\delta^{15}N$: 0.0024 $\delta^{13}C$: 0.4902	t-test 0.9118/ Mann-Whitney 0.949	$\delta^{18}O_{ap}$: 0.934 $\delta^{13}C_{ap}$: 0.417
Female	10.8±0.6 (10 to 12.2) -17.7±0.5 (-18.4 to -16.6) n=10	0.712399 (0.709236-0.713785) n=8	-3.4±0.9 (-4.4 to -2.1) -10.2±2.4 (-12.8 to -6.4) n=6
Male	10.9±1.0 (8.7 to 12.4) -18.2±1.2 (-20 to -16) n=9	0.713669 (0.710287-0.716632) n=9	-4.2±0.9 (-5.4 to -3) -9.8±2.6 (-13 to -6.9) n=5
Statistical Comparison Female vs Male (p-value)	$\delta^{15}N$: 0.2474 $\delta^{13}C$: 0.1972	t-test 0.17/ Mann-Whitney 0.1434	$\delta^{18}O_{ap}$: 0.1653 $\delta^{13}C_{ap}$: 1
Teeth	11.2±0.8 (10.4 to 12.7) -16.5±0.8 (-17.8 to -15.5) n=9	0.713132 (0.709236-0.716632) n=26	-4.0±1.0 (-6.5 to -2.1) -10.2±2.2 (-14.2 to -6.4) n=17
Ribs	10.9±0.6 (10.3 to 12.1) -17.6±0.4 (-18.2 to -16.6) n=9	-	-
Statistical Comparison Teeth vs Ribs (p-value)	$\delta^{15}N$: 0.5313 $\delta^{13}C$: 0.0076	-	-
Non-Local	11±0.7 (10.3 to 12.2) -17.8±1.1 (-20 to -16) n=8	0.714559 (0.713249-0.716632) n=12	-4.3±1.3 (-6.5 to -2.1) -10.5±2.4 (-16.0 to -8.4) n=8
Local	10.5±0.8 (8.7 to 11.5) -18.0±0.9 (-19.8 to -16.6) n=9	0.711910 (0.709236-0.712975) n=14	-3.7±0.6 (-4.4 to -2.9) -10.2±2.9 (-14.2 to -6.4) n=9
Statistical Comparison Local vs Non-local (p-value)	$\delta^{15}N$: 0.2857 $\delta^{13}C$: 0.3014	-	$\delta^{18}O_{ap}$: 0.1065 $\delta^{13}C_{ap}$: 0.9602
Total	10.9±0.8 (8.7 to 12.3) -17.8±0.8 (-20 to -16) n=25	0.713132 (0.709236-0.716632) n=26	-4.0±1.0 (-6.5 to -2.1) -10.2±2.2 (-14.2 to -6.4) n=17
Statistical Comparison Human vs Domestic Fauna from Rocha Forte (p-value)	-	-	$\delta^{18}O_{ap}$: 0.3198 $\delta^{13}C_{ap}$: 0.0003

Table S5. $\delta^{15}N$ and $\delta^{13}C$ statistical comparison (p-value) between tomb typologies

Tombs typology Comparison	Sarcophagus	Cists	Anthropomorphic	Rectangular
Sarcophagus	-	$\delta^{15}N$: 0.2014 $\delta^{13}C$: 1	$\delta^{15}N$: 0.7027 $\delta^{13}C$: 0.9126	$\delta^{15}N$: 1 $\delta^{13}C$: 0.8095
Cists	$\delta^{15}N$: 0.2014 $\delta^{13}C$: 1	-	$\delta^{15}N$: 1 $\delta^{13}C$: 1	$\delta^{15}N$: 1 $\delta^{13}C$:
Anthropomorphic	$\delta^{15}N$: 1 $\delta^{13}C$: 0.9126	$\delta^{15}N$: 1 $\delta^{13}C$: 1	-	$\delta^{15}N$: 1 $\delta^{13}C$: 1
Rectangular	$\delta^{15}N$: 1 $\delta^{13}C$: 0.8095	$\delta^{15}N$: 1 $\delta^{13}C$: 1	$\delta^{15}N$: 1 $\delta^{13}C$: 1	-
Kruskal-Wallis test for equal medians (p-values) $\delta^{15}N$: 0.1071 $\delta^{13}C$: 0.2728				

Table S6. $\delta^{13}C$ and $\delta^{15}N$ stable isotope ratios, collagen quality indicators, and species identification of fauna analysed at the present study

Reference	Place	Chronology	Species	δ15N (‰)	δ13C (‰)	N%	C%	C/N	Collagen Yield (%)
NCS(FAU)01	Cathedral Santiago (Santiago de Compostela, Galicia)	9^{th}-12^{th} centuries AD	*Bos taurus*	4.6	-21.2	14.4	39.1	3.2	16.9
NCS(FAU)02	Cathedral Santiago (Santiago de Compostela, Galicia)	9^{th}-12^{th} centuries AD	*Bos taurus*	3.9	-21.6	15.6	42.6	3.2	17.8
NCS(FAU)04	Cathedral Santiago (Santiago de Compostela, Galicia)	9^{th}-12^{th} centuries AD	Ovicaprine	5.2	-21.5	11.9	32.9	3.2	20.6
NCS(FAU)08	Cathedral Santiago (Santiago de Compostela, Galicia)	9^{th}-12^{th} centuries AD	*Bos taurus*	5.4	-21.3	13.4	36.5	3.2	3.5
NCS(FAU)09	Cathedral Santiago (Santiago de Compostela, Galicia)	9^{th}-12^{th} centuries AD	Ovicaprine	4.8	-21.4	17.0	45.7	3.1	13.6
NCS(FAU)010	Cathedral Santiago (Santiago de Compostela, Galicia)	9^{th}-12^{th} centuries AD	Ovicaprine	4.9	-21.4	12.5	34.1	3.2	2.4
NCS(FAU)012	Cathedral Santiago (Santiago de Compostela, Galicia)	9^{th}-12^{th} centuries AD	*Bos taurus*	4.5	-21.3	13.5	36.7	3.2	2.9
NCS(FAU)013	Cathedral Santiago (Santiago de Compostela, Galicia)	9^{th}-12^{th} centuries AD	*Bos taurus*	5.4	-21.3	13.4	37.0	3.2	5.3
NCS(FAU)014	Cathedral Santiago (Santiago de Compostela, Galicia)	9^{th}-12^{th} centuries AD	Ovicaprine	5.6	-21.4	13.2	36.3	3.2	15.1
ROCHA-OVI	Rocha Forte Castle (Santiago de Compostela, Galicia)	13^{th}-15^{th} centuries AD	Ovicaprids	8.8	-22.2	12.1	33.4	3.2	7.4
ROCHA-SUS	Rocha Forte Castle (Santiago de Compostela, Galicia)	13^{th}-15^{th} centuries AD	*Sus scrofa*	8.7	-19.6	13.4	36.5	3.2	11.3
ROCHA-BOS	Rocha Forte Castle (Santiago de Compostela, Galicia)	13^{th}-15^{th} centuries AD	*Bos taurus*	5.6	-21.8	14.0	37.9	3.1	8.6
RF(FAU)MO-25/9	Rocha Forte Castle (Santiago de Compostela, Galicia)	13^{th}-15^{th} centuries AD	*Bos taurus*	5.9	-22.1	13.2	37.0	3.3	3.2
RF(FAU)MO-65	Rocha Forte Castle (Santiago de Compostela, Galicia)	13^{th}-15^{th} centuries AD	Ovicaprine	5.5	-21.2	15.8	43.7	3.2	5.4
RF(FAU)MO-35	Rocha Forte Castle (Santiago de Compostela, Galicia)	13^{th}-15^{th} centuries AD	Ovicaprine	6.7	-22.3	15.0	43.7	3.4	2.6
MO-65/1	Rocha Forte Castle (Santiago de Compostela, Galicia)	13^{th}-15^{th} centuries AD	Ovicaprine?	8.8	-21.6	16.3	45.5	3.3	17.2
MO-29/4	Rocha Forte Castle (Santiago de Compostela, Galicia)	13^{th}-15^{th} centuries AD	Ovicaprine	6.9	-22.2	15.8	44.7	3.3	3.2
MO-02/1y2	Rocha Forte Castle (Santiago de Compostela, Galicia)	13^{th}-15^{th} centuries AD	*Merlucciiae*	13.0	-13.0	14.9	41.8	3.3	3.9

MO-25/7	Rocha Forte Castle (Santiago de Compostela, Galicia)	13^{th}-15^{th} centuries AD	*Sus scrofa*	8.5	-19.7	15.7	44.2	3.3	7.4
RF(GAL)FAU069	Rocha Forte Castle (Santiago de Compostela, Galicia)	13^{th}-15^{th} centuries AD	Ovicaprine	6.2	-22	14.0	41.1	3.4	6.3
MO-25/11	Rocha Forte Castle (Santiago de Compostela, Galicia)	13^{th}-15^{th} centuries AD	*Sus scrofa*	9.1	-18.5	14.9	41.2	3.2	8.1
MO-44	Rocha Forte Castle (Santiago de Compostela, Galicia)	13^{th}-15^{th} centuries AD	*Delphinidae*	11.9	-11.9	16.5	45.2	3.2	5.3
MO25/10	Rocha Forte Castle (Santiago de Compostela, Galicia)	13^{th}-15^{th} centuries AD	Ovicaprine	5	-21.8	10.5	28.8	3.2	3.5
MO61/4	Rocha Forte Castle (Santiago de Compostela, Galicia)	13^{th}-15^{th} centuries AD	*Bos taurus*?	6.1	-21.8	16.3	44.8	3.2	7.1
MO68/4	Rocha Forte Castle (Santiago de Compostela, Galicia)	13^{th}-15^{th} centuries AD	*Bos taurus*	6	-21.9	11.6	32.8	3.3	3.7
MO69/8	Rocha Forte Castle (Santiago de Compostela, Galicia)	13^{th}-15^{th} centuries AD	Ovicaprine	4,7	-21.7	16.3	44.4	3.2	2.0

Table S7. Statistical comparison between species from Rocha Forte Castle (Kruskall-Wallis and Mann-Whitney pairwise with Bonferroni correction) illustrating the p-value

Rocha Forte Fauna	***Bos taurus* (n = 8)**	**Ovicaprine (n = 14)**	***Sus scrofa* (n = 5)**	***Cervus elaphus* (n = 2)**
***Bos taurus* (n = 8)**	-	$\delta^{15}N$: 1 $\delta^{13}C$: 0.8157 $\delta^{13}C_{ap}$: 1	$\delta^{15}N$: 0.1555 $\delta^{13}C$: 0.04975 $\delta^{13}C_{ap}$: 0.311	$\delta^{13}C_{ap}$: 1
Ovicaprine (n = 14)	$\delta^{15}N$: 1 $\delta^{13}C$: 0.8157 $\delta^{13}C_{ap}$: 1	-	$\delta^{15}N$: 0.5773 $\delta^{13}C$: 0.01604 $\delta^{13}C_{ap}$: 0.1902	$\delta^{13}C_{ap}$: 1
***Sus scrofa* (n = 5)**	$\delta^{15}N$: 0.1555 $\delta^{13}C$: 0.04975 $\delta^{13}C_{ap}$: 0.311	$\delta^{15}N$: 0.5773 $\delta^{13}C$: 0.01604 $\delta^{13}C_{ap}$: 0.1902	-	$\delta^{13}C_{ap}$: 0.8935
***Cervus elaphus* (n = 2)**	$\delta^{13}C_{ap}$: 1	$\delta^{13}C_{ap}$: 1	$\delta^{13}C_{ap}$: 0.8935	
$\delta^{15}N$: 0.1162 $\delta^{13}C$: 0.03023 $\delta^{13}C_{ap}$: 0.08106				

Table S8. Summary data (range, mean, standard deviation, and number of samples) $\delta^{13}C$ and $\delta^{15}N$ measurements of fauna present study and statistical comparison (Mann-Whitney test with Monte-Carlo permutation) between species and origin

	Bos taurus	Ovicaprine	Total (without *Sus scrofa*)	Statistical Comparison species (p-value)
Cathedral of Santiago	4.8±0.6 (3.9 to 5.4) -21.3±0.1 (-21.6 to -21.2) n=5	5.1±0.4 (4.8 to 5.6) -21.4±0.1 (-21.5 to -21.4) n=4	4.9±0.5 (3.9 to 5.6) -21.4±0.1 (-21.6 to -21.2) n=9	$\delta^{15}N$: 0.3651 $\delta^{13}C$: 0.1995
Rocha Forte Castle	5.9±0.2 (5.6 to 6.1) -21.9±0.1 (-22.1 to -21.8) n=4	6.6±1.6 (4.7 to 8.8) -21.8±0.4 (-22.3 to -21.2) n=8	6.4±1.3 (4.7 to 8.8) -21.9±0.3 (-22.3 to -21.2) n=12	$\delta^{15}N$: 0.5466 $\delta^{13}C$: 1
Total (without *Sus scrofa*)	5.3±0.8 (3.9 to 6.1) -21.6±0.3 (-22.1 to -21.2) n=9	6.3±1.6 (4.7 to 8.8) -21.7±0.4 (-22.3 to -21.2) n=13	5.7±1.2 (3.9 to 8.8) -21.6±0.4 (-22.3 to -21.2) n=21	$\delta^{15}N$: 0.2533 $\delta^{13}C$: 0.4534
Statistical comparison origin (p-value)	$\delta^{15}N$: 0.0078 $\delta^{13}C$: 0.0178	$\delta^{15}N$: 0.1028 $\delta^{13}C$: 0.1954	$\delta^{15}N$: 0.0017 $\delta^{13}C$: 0.0032	-

S9. $^{87}Sr/^{86}Sr$ measurements (range) compiled from the literature across the Iberian Peninsula

Site	Substrate	Range	Reference
Tauste, Zaragoza, Spain (1)	Miocene materials around Tauste are composed of claystone with interbedded gypsum layers. These materials correspond to evaporite lacustrine facies	0.70843-0.70869	Guede *et al*. 2017
Bolores, Extremadura, Portugal	Rifting phase and the late Triassic. Cretaceous and Jurassic sediments with pockets of Triassic deposits. It is composed of heterogenous lithologies: limestones, sandstones, clays, marls, basalts, and volcanic rocks.	0.7090750-0.713280	Waterman *et al*. 2013
Zanbujal, Extremadura, Portugal	Rifting phase and the late Triassic. Cretaceous and Jurassic sediments with pockets of Triassic deposits. It is composed of heterogenous lithologies: limestones, sandstones, clays, marls, basalts, and volcanic rocks.	0.705502-0.711643	Waterman *et al*. 2013
Northern Sierras and Tagus River basin, Madrid región.	Cenozoic, out of igneous and metamorphic rocks of Paleozoic granite shelf plateau. Tagus: composed by detrital rocks (sand and marls) with some chemical and lacunar facies (gypsum and limestones)	0.707 to 0.713	Díaz-del-Río *et al*. 2017
Las Gobas, Treviño Burgos, Spain	Carbonate sedimentary rocks, mainly dolostones, and limestones	0.70784 to 0.70813	Guede *et al*. 2018
Alegria-Dulantzi	Cretaceous and Paleogene: limestone, marls, gravels, sands, and clays.	0.70778 to 0.70795	Ortega *et al*. 2013
Pamplona, Navarre	Silurian to Permian and Cretaceous. Carbonate and detrital sedimentary rocks	0.71119 to 0.712	Prevedouro *et al*. 2010
Alto de Reinoso, Burgos	gray-white facies, typical of the upper Miocene, giving an alternation of lakes and lake limestones	0.70918-0.70952	Kurt *et al*. 2016
Loarre, Huesca	Cretaceous-Miocene, limestone	0.708249-0.709984	Villalba-Mouco *et al*. 2018
Caravaca de la Cruz, Murcia	Mesozoic age sedimentary rock. Internal and external composed. Triassic-Miocene sedimentary rocks, including	0.707846-0.711588	Merner 2017

	limestones, marlstone, and sandstone.		
Marroquíes, Jaén	Jurassic limestone and cretaceous loan	0.70675-0.71020	Díaz-Zorita Bonilla *et al*. 2018
La Pijotilla, Solana de los Barros, Badajoz	Tertiary soils corresponding to the Miocene, formed by arches, sandstones, and microconglomerates sometimes with carbonated	0.714175-0.715382	Díaz-Zorita *et al*. 2018
Valencina de la Concepción y Castilleja de Guzmán, Sevilla	Tertiary soils, composed of sandy silts and in some areas by brown loam and sand	0.708644-0.709323	Díaz-Zorita *et al*. 2018
Avinyonet del Penedés, Barcelona	Miocene sediments	0.7094-0.7096	Valenzuela-Lamas *et al*. 2016
Pico Ramos, Bilbao,	Lower Cretaceous substrate. Albian-Aptian.	0.70748-0.7079	Sarasketa-Gartzia *et al*. 2018

Table S10. Summary data (range, mean, standard deviation, and number of samples) $\delta^{13}C$ and $\delta^{15}N$ measurements of human northern medieval Christians compiled from the literature

Site, location, and chronology	$\delta^{13}C$ (‰) and $\delta^{15}N$ (‰) Mean ± SD, Range and number of samples	Reference
Capela do Pilar, Santa María Cathedral (Lugo, Galicia) 12th-15th centuries AD	13.6±1.3 (11.3 to 15.7) -18.6 ± 0.5 (-19.4 to -17.9) n = (9)	Kaal *et al*., 2016; and López-Costas *et al*. 2021
San Bartolomé, (Pontevedra, Galicia) 13th-15th centuries AD	11.7±1.0 (12.9 to 9.9) -16.9 ± 1.0 (-15.2 to -18.7) n = (16)	López-Costas and Müldner 2018
São Jorge (Lisbon, Portugal) 11th-12th centuries AD	9.9±0.8 (8.9 to 11.2) -18.9±0.3 (-19.4 to -18.5) n = (27)	Toso *et al*. 2019
Chao Samartín (Grandas Salime, Asturias) 8th-15th centuries AD	10.1±0.6 (9.6 to 11.4) -18.8±0.5 (-19.3 to -17.8) n = (6)	MacKinnon *et al*. 2019
San Pedro Nora (Las Regueras, Asturias) 12th-15th centuries AD	10.3±1 (8.8 to 11.3) -18.3±1.9 (-19.8 to -13.1) n = (12)	MacKinnon *et al*. 2019
San Salvador Cathedral (Oviedo, Asturias) 10th centuries AD	12.0±1.2 (10.3 to 13) -18.6 ± 0.2 (-19.9 to -18.4) n = (4)	MacKinnon *et al*. 2019
San Miguel de Lillo (Oviedo, Asturias) 12th-15th centuries AD	10.4±1.1 (9.2 to 13.9) -17.6±2.5 (-19.5 to -10.7) n = (16)	MacKinnon *et al*. 2019
San Salvador de Valdedios (Villaviciosa, Asturias) 10th-14th centuries AD	9.7±0.8 (8.8 to 12.2) -19.0±0.8 (-19.6 to -18.0) n = (12)	MacKinnon *et al*. 2019
Zaballa Nanclares de la Oca (Álava, Basque Country) 10th-15th centuries AD	9.4±1.3 (7.6 to 12.5) -19.9±0.9 (-22.3 to -18.8) n = (14)	Lubritto *et al.* 2017

EM Dulantzi Alegría-Dulantzi (Álava, Basque Country) 8th-12th centuries AD	9.1±1.2 (4.7 to 12.2) -18.8 ± 1.4 (-24.5 to -14.1) n = (45)	Lubritto *et al.* 2017
EM Aistra Zalduondo (Álava, Basque Country) 8th-10th centuries AD	8±1.1 (6.7 to 12.1) -18.9 ± 1 (-22 to -16.7) n = (44)	Lubritto *et al.* 2017
Zornoztegi Salvatierra-Agurain (Álava, Basque Country) 12th-14th centuries AD	8.0±0.6 (7 to 9.2) -18.2 ± 0.8 (-19.9 to -17.2) n = (9)	Lubritto *et al.* 2017
Treviño, Condado de Treviño (Burgos, Castile and León) 12th-15th centuries AD	9.6±1.1 (7.5 to 12) -19.5±0.7 (-22 to -18.7) n = (19)	Lubritto *et al.* 2017
Las Gobas Treviño, Burgos (Castile and León) 7th-11th centuries AD	8.9±0.9 (7.7 to 11.7) -19 ± 0.6 (-20.1 to -17.2) n = (40)	Guede *et al*. 2018
Castile Royal Family, Virgen de los Reyes chapel, Santa María de la Sede Cathedral (Seville, Andalusia)** 14th century AD	13.3±1.5 (11.9 to 15.6) -18.6 ± 0.5 (-19.3 to -18.0) n = (5)	Jiménez-Brobeil *et al*. 2016

***=Sub-adults are excluded. **=these individuals were combined as all of them were born and spent most of their lives in this part of the Iberian Peninsula despite burial elsewhere**

References

Alt KW, Zesch S, Garrido-Pena R, Knipper C, Szécsényi-Nagy A, Roth C, Tejedor-Rodríguez C, Held P, García-Martínez-De-Lagrán Í, Navitainuck D, Magallón HA, Rojo-Guerra MA (2016) A community in life and death: The late neolithic megalithic tomb at Alto de Reinoso (Burgos, Spain). PLoS One 11(1): e0146176.

Araguas-Araguasa LJ, Diaz Teijeiro MF (2005) Isotope composition of precipitation and water vapour in the Iberian Peninsula. First results of the Spanish network of isotopes in precipitation. Isotopic composition of precipitation in the Mediterranean Basin in relation to air circulation patterns and climate. International Atomic Energy Agency, Isotope Hydrology Section: 173–190.

Beaumont J, Gledhill A, Lee-Thorp J, Montgomery JA (2013) Childhood diet: a closer examination of the evidence from dental tissues using stable isotope analysis of incremental human dentine. Archaeometry *55*(2): 277–295.

Bronk Ramsey C (2017) Methods for summarizing radiocarbon datasets. Radiocarbon 59(6): 1809–1833. doi:10.1017/RDC.2017.108.

Bronk Ramsey C, Higham TFG, Leach P (2004) Towards high-precision AMS: progress and limitations. Radiocarbon 46(1): 17-24.

Brock F, Higham T, Ramsey CB (2010) Pre-screening techniques for identification of samples suitable for radiocarbon dating of poorly preserved bones. J Archaeol Sci 37(4): 855-865. doi:10.1016/j.jas.2009.11.015.

Brown TA, Nelson DE, Vogel JS, Southon JR (1988) Improved Collagen Extraction by Modified Longin Method. Radiocarbon 30(2): 171-177.

Díaz-del-Río P, Waterman AJ, Thomas JT, Peate DW, Tykot RH, Martínez-Navarrete MI, Vicent JM (2017) Diet and mobility patterns in the Late Prehistory of central Iberia (4000–1400 cal bc): the evidence of radiogenic ($^{87}Sr/^{86}Sr$) and stable ($\delta^{18}O$, $\delta^{13}C$) isotope ratios. Archaeol Anthropol Sci 9(7): 1439–1452. doi:10.1007/s12520-017-0480-y.

Díaz-Zorita Bonilla M, Beck J, Bocherens H, Díaz-del-Río P (2018) Isotopic evidence for mobility at large-scale human aggregations in Copper Age Iberia: the mega-site of Marroquíes. Antiquity 92(364): 991–1007. doi:10.15184/aqy.2018.33.

Guede I, Ortega LA, Cruz Zuluaga M, Alonso-Olazabal A, Murelaga X, Pina M, Gutierrez FJ, Iacumin P (2017) Isotope analyses to explore diet and mobility in a medieval Muslim population at Tauste (NE Spain). PLoS One 12(5): e0176572. doi:10.1371/journal.pone.0176572.

Guede I, Ortega LA, Cruz Zuluaga M, Alonso-Olazabal A, Murelaga X, Solaun JL, Sanchez I, Azkarate A (2018) Isotopic evidence for the reconstruction of diet and mobility during village formation in the Early Middle Ages: Las Gobas (Burgos, northern Spain). Archaeol Anthropol Sci 10(8): 2047–2058. doi:10.1007/s12520-017-0510-9.

Higham T, Ramsey CB, Karavanić I, Smith FH, Trinkaus E (2006) Revised direct radiocarbon dating of the Vindija G1 Upper Paleolithic Neandertals. Proc Natl Acad Sci USA 103(3): 553-557. doi:10.1073/pnas.0510005103.

Jacob E, Querci D, Caparros M, Barroso Ruiz C, Higham T, Devièse T (2018) Nitrogen content variation in archaeological bone and its implications for stable isotope analysis and radiocarbon dating. J Archaeol Sci 93: 68–73.

Jiménez-Brobeil SA, Laffranchi Z, Maroto RM, López Sánchez FA, Delgado Huertas A (2016) How royals feasted in the court of Pedro I of Castile: A contribution of stable isotope study to medieval history. J Archaeol Sci Reports 10: 424–430. doi:10.1016/j.jasrep.2016.11.010.

Kaal J, López-Costas O, Martínez Cortizas A (2016) Diagenetic effects on pyrolysis fingerprints of extracted collagen in archaeological human bones from NW Spain, as determined by pyrolysis-GC-MS. J Archaeol Sci 65: 1–10. doi:10.1016/j.jas.2015.11.001.

López-Costas O, Müldner G, Lidén K (2021) Biological histories of an elite: Skeletons from the Royal Chapel of Lugo Cathedral (NW Spain). Int J Osteoarchaeol 31: 941-956 doi:10.1002/oa.3011.

López-Costas O, Müldner, G (2018) Boom and bust at a medieval fishing port: Dietary preferences of fishers and artisan families from Pontevedra (Galicia, NW Spain) during the Late Medieval and Early Modern Period. Archaeol Anthropol Sci 11(8), 3717–3731. Doi: 10.1007/s12520-018-0733-4.

Lubritto C, García-Collado MI, Ricci P, Altieri S, Sirignano C, Quirós Castillo JA (2017) New dietary evidence on medieval rural communities of the Basque Country (Spain) and its surroundings from carbon and nitrogen stable isotope analyses: Social insights, diachronic changes and geographic comparison. Int J Osteoarchaeol 27(6), 984–1002. doi:10.1002/oa.2610.

MacKinnon AT, Passalacqua NV, Bartelink EJ (2019) Exploring diet and status in the Medieval and Modern periods of Asturias, Spain, using stable isotopes from bone collagen. Archaeol Anthropol Sci 11(3), 3837–3855.

Merner C (2017) Reconstructing Southeast Iberian copper age mobility: a strontium isotope analysis of the Camino del Molino mass burial. Master thesis: University of Newfoundland.

Ortega LA, Guede I, Zuluaga, M.C., Alonso-Olazabal, A., Murelaga, X., Niso, J., Loza, M, J.A. Quirós Castillo (2013) Strontium isotopes of human remains from the San Martín de Dulantzi graveyard (Alegría-Dulantzi, Álava) and population mobility in the Early Middle Ages." Quat Int 303: 54–63.

Pérez Ramallo P (2015) Pilgrimage to Santiago de Compostela: Investigating society and the geographical mobility of medieval individuals. Master Dissertation. Universirty of Bradford, Bradford, the UK.

Prevedorou E, Bonilla MD-Z, Romero A, Buikstra JE, Ibáñez MP de M, Knudson KJ (2018) Residential Mobility and Dental Decoration in Early Medieval Spain: Results from the Eighth

Century Site of Plaza del Castillo, Pamplona. Dent Anthropol J 23: 45-52. doi:10.26575/daj.v23i2.74.

Ramsey CB, Higham T, Leach P (2004) Towards high-precision AMS: Progress and limitations. Radiocarbon. doi:10.1017/s0033822200039308.

Ramsey CB (2017) Methods for Summarizing Radiocarbon Datasets. Radiocarbon 59(6): 1809-1833doi:10.1017/RDC.2017.108.

Reimer PJ, Austin WEN, Bard E, Bayliss A, Blackwell PG, Bronk Ramsey C, Butzin M, Cheng H, Edwards RL, Friedrichet, M. et al. (2020). The IntCal20 Northern Hemisphere Radiocarbon Age Calibration Curve (0-55 cal kBP). Radiocarbon 62(4), 725–757. doi:10.1017/RDC.2020.41.

Sarasketa-Gartzia I, Villalba-Mouco V, le Roux P, Arrizabalaga Á, Salazar-García DC (2018) Late Neolithic-Chalcolithic socio-economical dynamics in Northern Iberia. A multi-isotope study on diet and provenance from Santimamiñe and Pico Ramos archaeological sites (Basque Country, Spain). Quat Int 481: 14–27. doi:10.1016/j.quaint.2017.05.049.

Toso A, Gaspar S, Banha da Silva R, Garcia SJ, Alexander M (2019) High status diet and health in Medieval Lisbon: A combined isotopic and osteological analysis of the Islamic population from São Jorge Castle, Portugal. Archaeol Anthropol Sci 11: 3699–3716. doi:10.1007/s12520-019-00822-7.

Valenzuela-Lamas S, Jiménez-Manchón S, Evans J, López D, Jornet R, Albarella U (2016) Analysis of seasonal mobility of sheep in Iron Age Catalonia (north-eastern Spain) based on strontium and oxygen isotope analysis from tooth enamel: First results. J Archaeol Sci Rep 6: 828-836. doi:10.1016/j.jasrep.2015.08.042.

Villalba-Mouco V, Sauqué V, Sarasketa-Gartzia I, Pastor MV, le Roux PJ, Vicente D, et al. (2018) Territorial mobility and subsistence strategies during the Ebro Basin Late Neolithic-Chalcolithic: A multi-isotope approach from San Juan cave (Loarre, Spain). Quat Int 481, 28-41. doi:10.1016/j.quaint.2017.05.051.

Waterman AJ, Peate DW, Silva AM, Thomas JT (2014) In search of homelands: Using strontium isotopes to identify biological markers of mobility in late prehistoric Portugal. J Archaeol Sci 28, 119–127. doi:10.1016/j.jas.2013.11.004.